

## Observation of Manakov Spatial Solitons in AlGaAs Planar Waveguides

J. U. Kang and G. I. Stegeman

*Center for Research and Education in Optics and Lasers (CREOL), University of Central Florida,  
12424 Research Parkway, Orlando, Florida 32826*

J. S. Aitchison

*Department of Electronics and Electrical Engineering, University of Glasgow,  
Glasgow G12 8LT, United Kingdom*

N. Akhmediev

*Optical Sciences Center, The Australian National University,  
Canberra, ACT0200, Australia  
(Received 4 December 1995)*

We suggest and implement a method for observing Manakov spatial solitons in crystals. We show experimentally that the propagation behavior of mutually trapped, orthogonally polarized beams in AlGaAs planar waveguides is identical to that of a fundamental (single polarization) soliton beam with the same total power. [S0031-9007(96)00140-8]

PACS numbers: 42.65.Tg

The self-focusing and guiding of an intense electromagnetic wave in a nonlinear medium has inspired curiosity and interest since the earliest days of nonlinear optics [1]. However, it was not until the work of Zakharov and Shabat [2] that a clear connection between these phenomena and soliton theory was made. They developed the inverse scattering method for solving the nonlinear Schrödinger equation (NLS) and were able to solve the initial value problem analytically. Extending the inverse scattering technique to  $3 \times 3$  matrix equations [3], Manakov integrated the coupled nonlinear Schrödinger equations which describe the propagation of optical beams with two orthogonal polarizations. In reality, the equations which determine the propagation of an optical beam in a one-dimensional self-focusing medium are more complicated and not always integrable. There are certain conditions for integrability of these equations [4]. Namely, for the coupled set of equations with cubic nonlinearity the conditions of integrability are twofold: the ratio between the self-phase modulation (SPM) to the cross-phase modulation (XPM) has to be equal to unity and the SPM coefficients need to be equal for the two polarizations. Moreover, the energy exchange terms, sometimes known as the four wave mixing (FWM) terms, must be zero. Integrability gives certain advantages for soliton propagation. In particular, the prescribed way of soliton interaction, the absence of energy transfer from solitons into radiation modes during the collision and even during propagation [5] are the most important.

There are no crystal symmetries which *a priori* lead to a SPM/XPM ratio of unity. Hence, this condition depends on the detailed physics of a given material. For example, this ratio is 3/2 in isotropic media such as fused quartz. Hence, Manakov solitons cannot be observed in standard optical fibers [6]. Our studies have indicated that in AlGaAs, for photon energies just

below half the band gap, the ratio is just less than unity (to within the experimental error) [6,7] and also the nonlinear coefficients for the transverse electric fields of the TE mode ( $E \parallel 110$ ) and the TM mode ( $E \parallel 001$ ) are approximately the same. However, the FWM terms in the coupled NLS always exist. The presence of these terms can completely change the beam behavior relative to the solitonlike one. Although stationary beam solutions via "solitary waves," called vector solitons by Christodoulides and Joseph [8], may exist, the propagation of such beams can be unstable [5]. Moreover, these terms can even turn the dynamics of wave propagation into chaos [9].

Two ways to arrange Manakov conditions in real materials are known today. For pulses in optical fibers, it has been shown by Menyuk [10] that the FWM terms can be averaged to zero in strongly birefringent fibers due to the fast phase changes between the linearly polarized components. This is caused by the large wave-vector mismatch between the two polarization components of the soliton. However, the fiber must be designed in a special way to turn the SPM to XPM ratio to unity [11]. Another possible way is to use a randomly birefringent fiber [12]. In the latter case, the averaging of the state of polarization over the Poincaré sphere also reduces the governing equations for an isotropic material to the Manakov case. But this cannot be done in cubic crystals because of the lack of the above symmetry condition. The aim of this work is to suggest different experimental conditions in which the beam propagation can follow Manakov equations in the spatial domain in order to observe solitons experimentally in the strict mathematical sense.

The propagation of optical beams in terms of the two orthogonal modes of a planar waveguide where the beams are only allowed to diffract in one spatial dimension can be written as [10]

$$\frac{\partial E_e}{\partial z} = \frac{i}{2k} \frac{\partial^2 E_e}{\partial x^2} + ik_0 n_2 [|E_e|^2 E_e + A |E_m|^2 E_e + B E_m^2 E_e^* \exp(-i2\delta kz)],$$

$$\frac{\partial E_m}{\partial z} = \frac{i}{2k} \frac{\partial^2 E_m}{\partial x^2} + ik_0 n_2 [|E_m|^2 E_m + A |E_e|^2 E_m + B E_e^2 E_m^* \exp(i2\delta kz)],$$

where  $E_e$  and  $E_m$  are the transverse electric fields for the TE and TM modes, respectively,  $k_0$  is the propagation constant in the vacuum,  $n_2$  is the nonlinear refractive index coefficient for both polarizations,  $A$  is the ratio between the cross- and self-phase modulation coefficients,  $B$  is the ratio between XPM and FWM, and  $\delta k$  is the wave-vector mismatch defined as  $k_0(n_e - n_m)$ , with  $n_e$  and  $n_m$  the effective indices for the TE and TM guided wave fields, respectively. In the waveguide, which we are using,  $n_e - n_m$  is below 0.0007. For power levels of our experiment, the linear beat length and nonlinear beat length are comparable and FWM terms cannot be simply removed.

Depending on the values of  $A$  and  $B$  and on the total pulse power, these equations have two, four, or six stationary solutions (fixed points) in the form of elliptically polarized spatial vector solitons. If  $B = 1 - A$  (for isotropic media), the number of fixed points can be two or four [8]. The beam behavior and the evolution of its state of polarization are defined by the interlocation of these fixed points on the Poincaré sphere and can be quite complicated in general. If we neglect the FWM (last) terms ( $B = 0$ ) and if  $A$  is unity, the equations reduce to the Manakov generating equations and the beam propagation behavior becomes different. Note that the soliton interaction in the presence of the FWM terms is also different from the interaction of fundamental solitons.

For both the single-component NLS and the two-component Manakov equations solitons are the so-called envelope solitons because the phase of the carrier does not play any role in soliton propagation. Although for real crystals the common phase can also be removed from the equations, the relative phase between the components is the parameter which plays a major role in the pulse dynamics. This means that mutual coherence or incoherence of the two components can completely change the pulse dynamics from one extreme to the other. This is the idea we are exploiting in this work to switch the behavior of solitons from one regime to another.

Note that the FWM terms cannot be simply ignored. However, if the two orthogonally polarized beams are incoherent relative to each other, they can be averaged and become equal to zero. Manakov equations conserve the power in each component separately. For two incoherent components, there is still energy exchange, but it is zero on average. In this paper, we show experimentally that the FWM term can be made effectively zero in AlGaAs, and we report the first observation of spatial Manakov solitons. The experiment is done in an AlGaAs

planar waveguide operating at a wavelength below half its band gap. Furthermore, we show experimentally that the propagation of Manakov solitons is similar to that of single polarization fundamental solitons [13].

The experiment was performed with a NaCl:OH<sup>-</sup> color center laser operating at a wavelength of 1.55  $\mu\text{m}$ . Using additive pulse mode locking (APM), the laser produces 670 fsec pulses at 76 MHz. An approximately 14 mm long planar AlGaAs waveguide was used which consisted of a 1  $\mu\text{m}$  thick guiding layer of Al<sub>0.18</sub>Ga<sub>0.82</sub>As, a 4  $\mu\text{m}$  thick lower cladding region of Al<sub>0.4</sub>Ga<sub>0.6</sub>As, and a 1.5  $\mu\text{m}$  thick upper cladding region of Al<sub>0.3</sub>Ga<sub>0.7</sub>As. The linear loss of this waveguide was measured to be 0.16 cm<sup>-1</sup> at the operating wavelength, negligible. Using a combination of a  $\lambda/2$  wave plate and a polarizing beam splitter, the input beam was separated into TE and TM beams. The rest of the experimental setup is shown schematically in Fig. 1. After a delay line, the two beams were recombined using a polarizing beam splitter. These beams were then elliptically shaped using a cylindrical telescope and end-fire coupled into the waveguide using a 20 $\times$  microscope objective. The output was imaged onto a camera using a 10 $\times$  microscope objective. Approximately 16  $\pm$  2  $\mu\text{m}$  ( $1/e^2$  radius) wide (in the plane of the waveguide) Gaussian beams were overlapped at the input facet and launched together, overlapped optimally in time and space. At the output, a polarizer was used to block the TE beam (or TM beam when appropriate) so that only the spatial profile of one beam could be recorded using an infrared camera.

At low input peak powers, both beams diffracted by about 8 times to 130  $\pm$  10  $\mu\text{m}$  as they propagated through the 14 mm long sample [14], i.e., the sample was approximately 8 diffraction lengths long. When each polarization was launched independently with a peak power of 550–600 W, a soliton with the same spatial width as the input beam emerged at the output. About 50 W more input peak power was required for the TM than the TE beams to achieve the same output beam width. We attribute this to different launch conditions, scattering

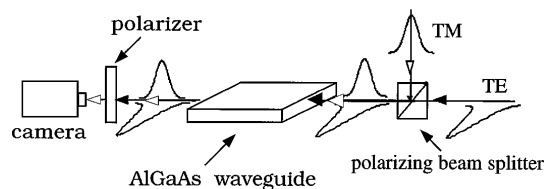


FIG. 1. Schematic of the experimental geometry.

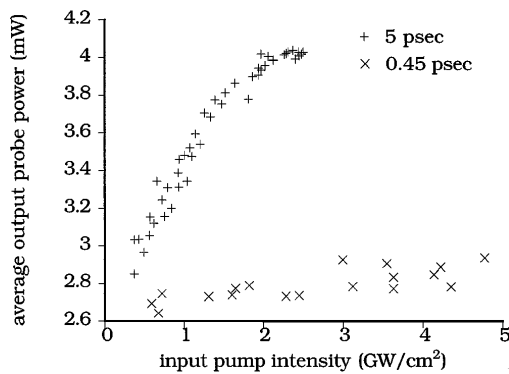


FIG. 2. Average TE signal output power as a function of TM pump input intensity for picosecond pulses (pluses) and femtosecond pulses (crosses).

losses, and perhaps an approximately 5% difference in  $n_2$ . In a channel waveguide, we measured the  $n_2$  coefficient for TE and TM polarizations to  $(1.5 \pm 0.1) \times 10^{-13}$  and  $(1.43 \pm 0.1) \times 10^{-13}$   $\text{cm}^2/\text{W}$ , respectively.

In an earlier experiment [15], we investigated power transfer between orthogonally polarized beams via the FWM effect in channel waveguides with a similar structure to this waveguide, but designed to have a smaller birefringence. The power transfer from a strong pump beam into an orthogonally polarized weak probe beam in the pump-probe setup was measured as a function of input pump intensity for both 5 and  $\sim 450$  fsec pulses. (In the pump-probe setup the beam is split into two polarizations which undergo different optical paths prior to entering the waveguide.) For zero phase difference between the TM pump and the TE probe, gain occurs for the TE probe in the 5 psec case; see Fig. 2. However, for the 450 fsec pulses, no change in the TE probe as a function of TM pump intensity was measured; that is, the FWM terms were not effective in this case. We repeated the experiment as a function of time delay and did not observe any change in the probe intensity. However, when we inputted a linearly polarized beam at some angle relative to the TM axis such that most of the power was in the TM mode, as a function of input intensity we observed strong power coupling from TM to TE for femtosecond pulses. We believe that the reason we did not observe FWM effects in the pump-probe setup using femtosecond pulses is because the delay line introduces significant chirp into femtosecond, TM polarized pulses so that the two beams are no longer coherent at the sample input. In such a case the FWM effect was zero, and this was the method used to eliminate the effects of FWM in these experiments.

A number of experiments were performed to verify that Manakov solitons were indeed generated. We first launched only a TE-polarized, fundamental, spatial soliton beam with an input power of  $\sim 550$  W, and the output was recorded and is shown in Fig. 3(a). Then we launched both TE and TM beams simultaneously with a power

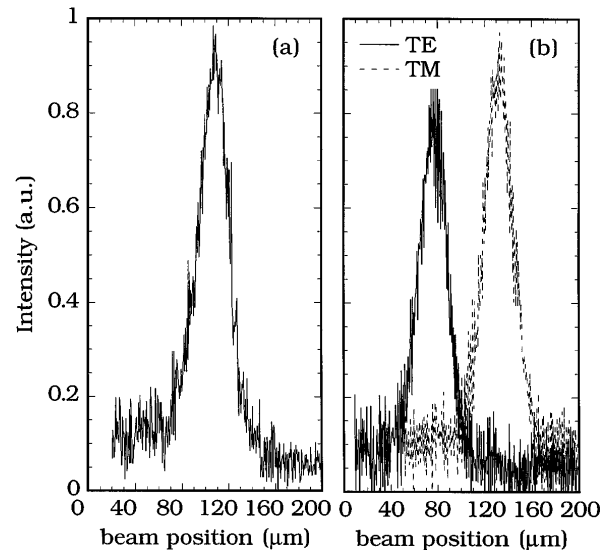


FIG. 3. Output beam profiles for (a) a TE fundamental soliton beam, (b) a Manakov soliton beam. The solid lines and dotted lines represent the TE and TM components, respectively.

ratio of about 1 to 2, but with a total power equal to that of the fundamental soliton just discussed. In this case, the two orthogonally polarized beams mutually trapped each other and copropagated through the sample. The output width and the shape of the two polarizations were identical [Fig. 3(b)], and the same as the fundamental soliton shown in Fig. 3(a). The two outputs in Fig. 3(b) actually overlap in space and were graphically shifted for easier comparison. A variable attenuator was used in front of the camera to ensure that the intensity level of all the beams imaged at the camera were the same. We repeated the experiment for different power ratios ranging from 1:20 and 20:1, but keeping the same total input power. For all the different power ratios the width and shape of the TE and TM beam did not change to within

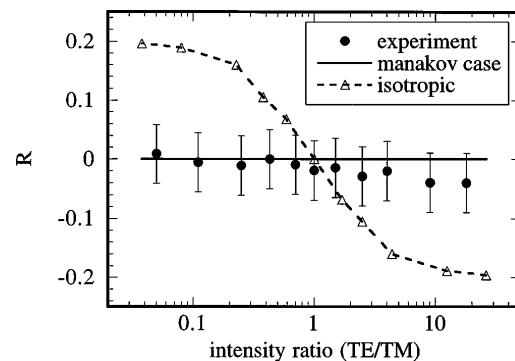


FIG. 4. The normalized difference between the output TE and TM beam widths [ $R = (\omega_{\text{TE}} - \omega_{\text{TM}})/\omega_{\text{TE}}$ ] versus the intensity ratio  $I_{\text{TE}}/I_{\text{TM}}$  of both beams, col launched at the input. The solid line is the Manakov prediction and the dashed line with triangle symbols is for an isotropic medium.

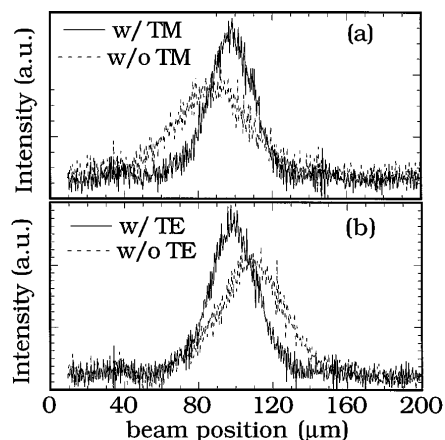


FIG. 5. (a) The output beam profile of TE solitons with (solid line) and without (dotted line) the TM soliton and (b) the output beam profile of TM solitons with (solid line) and without (dotted line) the TE soliton. The solid lines represent the Manakov soliton case.

the experimental uncertainty. The relative difference between the widths of the TE and TM beams at the output of the waveguide are shown graphically in Fig. 4, along with the theoretical curves for a “Manakov” and an isotropic material. These results are all consistent with the generation and propagation of Manakov solitons.

We also verified that the two orthogonally polarized beams are indeed mutually trapped. The two polarizations were initially overlapped at the input with equal powers and were launched at an angle of 0.1 deg relative to each other. Without the presence of the orthogonally polarized beam, each beam emerged at the output in the direction in which it was launched with a beam width of approximately 35  $\mu\text{m}$ , approximately twice the input beam width. However, when the beams are col launched, the two beams mutually trapped each other and copropagated through the sample, emerging at a common output in a direction which bisected the directions in which the beams were launched. The resulting beam width was equivalent to the width of a soliton beam with an intensity equal to the sum of the two individual input solitons, i.e., 18  $\mu\text{m}$ . Figure 5 illustrates these results. Note the significant decrease in the width of the TE soliton from approximately 35 to 18  $\mu\text{m}$  in the presence of the TM soliton. This shows the “robustness” of the launching conditions.

In conclusion, we have suggested and implemented a method for experimentally observing Manakov spatial

solitons. Namely, the two orthogonally polarized beams must be mutually incoherent so that the two beams are coupled only through XPM index potentials with no FWM term. In the experiment, we used an AlGaAs planar waveguide operating at a wavelength below half its band gap. For the same total input power, the output of this mutually trapped state of two orthogonally polarized solitons was identical to that of a fundamental, single-polarization soliton.

We acknowledge useful discussions with D. C. Hutchings. This research was supported by the U.S. NSF and in the U.K. by the SERC. J. S. A. acknowledges support from the Royal Society of Edinburgh/Scottish Office Education Department. N. A. acknowledges the Bede Morris Fellowship of Australian Academy of Sciences.

- 
- [1] For example, R. Y. Chiao, E. Garmire, and C. H. Towns, *Phys. Rev. Lett.* **13**, 479–482 (1964); P. L. Kelley, *Phys. Rev. Lett.* **15**, 1005 (1965).
  - [2] V. E. Zakharov and A. B. Shabat, *Sov. Phys. JETP* **34**, 62 (1972).
  - [3] S. V. Manakov, *Sov. Phys. JETP* **38**, 248 (1974).
  - [4] V. E. Zakharov and E. I. Schulman, *Physica (Amsterdam)* **4D**, 270 (1982).
  - [5] N. Akhmediev and J. M. Soto-Crespo, *Phys. Rev. E* **49**, 5742 (1994).
  - [6] D. C. Hutchings, J. S. Aitchison, B. S. Wherrett, G. T. Kennedy, and W. Sibbett, *Opt. Lett.* **20**, 991 (1995).
  - [7] A. Villeneuve, J. U. Kang, J. S. Aitchison, and G. I. Stegeman, *Appl. Phys. Lett.* **67**, 760 (1995).
  - [8] D. N. Christodoulides and R. I. Joseph, *Opt. Lett.* **13**, 53 (1988).
  - [9] D. David, D. D. Holm, and M. V. Tratnik, *Phys. Rep.* **187**, 281 (1990).
  - [10] C. R. Menyuk, *IEEE J. Quantum Electron.* **QE-23**, 174 (1987).
  - [11] C. R. Menyuk, *IEEE J. Quantum Electron.* **QE-25**, 2674 (1989).
  - [12] S. G. Evangelides, L. F. Mollenauer, and J. P. Gordon, *J. Lightwave Technol.* **10**, 28 (1992).
  - [13] J. S. Aitchison, Y. Silberberg, A. M. Weiner, D. E. Leaird, M. K. Oliver, J. L. Jackel, E. M. Vogel, and P. W. E. Smith, *J. Opt. Soc. Am. D* **8**, 1290 (1991).
  - [14] J. U. Kang, G. I. Stegeman, and J. S. Aitchison, *Opt. Lett.* **20**, 2069 (1995).
  - [15] J. S. Aitchison, J. U. Kang, and G. I. Stegeman, *Appl. Phys. Lett.* **67**, 2456 (1995).